Am J Cancer Res 2019;9(8):1650-1663
www.ajcr.us /ISSN:2156-6976/ajcr0097765

Original Article

LKB1 deficiency promotes proliferation and invasion of glioblastoma through activation of mTOR and focal adhesion kinase signaling pathways

Keqiang Zhang[1], Jinghan Wang[2], Jinhui Wang[3], Frank Luh[4], Xiyong Liu[4], Lu Yang[5], Yun-Ru Liu[6], Leila Su[4], Yu-Chen SH Yang[7], Peiguo Chu[8], Yun Yen[6,7,9,10]

[1]Department of Surgery, City of Hope National Medical Center, Duarte, CA, USA; [2]The First Department of Biliary Surgery, Eastern Hepatobiliary Surgical Hospital, Shanghai, China; [3]The Integrative Genomics Core Lab, City of Hope National Medical Center, Duarte, CA, USA; [4]Sino-American Cancer Foundation, Temple City, CA, USA; [5]Department of System Biology, City of Hope National Medical Center, Duarte, CA, USA; [6]Comprehensive Cancer Center, Taipei Medical University, Taipei, Taiwan; [7]PhD Program of Cancer Biology and Drug Discovery, College of Medical Science and Technology, Taipei Medical University, Taipei, Taiwan; [8]Department of Pathology, City of Hope National Medical Center, Duarte, CA, USA; [9]Research Center of Cancer Translational Medicine, Taipei Medical University, Taipei, Taiwan; [10]Graduate Institute of Cancer Biology and Drug Discovery, Taipei Medical University, Taipei, Taiwan

Received May 30, 2019; Accepted July 28, 2019; Epub August 1, 2019; Published August 15, 2019

Abstract: Liver kinase B1 (LKB1), a serine/threonine kinase, is frequently inactivated in several types of human cancers. To date, inactivation of LKB1 tumor suppressor has rarely been reported in glioblastoma. In this study, we investigated LKB1 status, biological significance, and therapeutic implications in glioblastoma. Loss of LKB1 immunostaining was identified in 8.6% (5/58), while decrease of LKB1 immunostaining was found in 29.3% (17/58) of glioblastoma tissues. Notably, mining TCGA database of LKB1 expression in glioblastoma revealed that lower mRNA level of LKB1 was associated with shorter survival in glioblastoma. We found that knockdown of LKB1 significantly promoted *in vitro* proliferation, adhesion, invasion, and metformin-induced apoptosis, and simultaneously enhanced activation of ERK and mammalian-target of rapamycin (mTOR) signaling pathways in LKB1-compenent U87 and T98 glioblastoma cells. Moreover, global transcriptional profiling revealed that adhesion and cytoskeletal proteins such as Vinculin, Talin and signaling pathways including focal adhesion kinase (FAK), extracellular martrix (ECM) receptor interaction, and cellular motility were significantly enriched in U87 and T98 glioblastoma cells upon LKB1 knockdown. Additionally, we demonstrated that the enhanced activation of FAK by LKB1 knockdown was dependent on differentially expressed cytoskeletal proteins in these glioblastoma cells. Importantly, we further found that mTOR1 inhibitor rapamycin dominantly inhibited *in vitro* cellular proliferation, while FAK inhibitor PF-573288 drastically decreased invasion of LKB1-attenuated glioblastoma cells. Therefore, downregulation of LKB1 may contribute to the pathogenesis and malignancy of glioblastoma and may have potential implications for stratification and treatment of glioblastoma patients.

Keywords: Glioblastoma, LKB1, focal adhesion kinase, cytoskeletal proteins, mTOR

Introduction

Glioblastoma, a grade IV glioma, is the most common and most aggressive primary malignant brain cancer in adults. Despite of advances in diagnosis and standard therapies (surgery, radiation, and chemotherapy), the prognosis of glioblastoma remains poor with a median survival of 12-15 months after diagnosis [1]. Infiltrating into normal brain parenchyma is one of the most fatal features of glioblastoma [2]. This aggressive characteristic of glioblastoma makes surgical resection very difficult and radiation and chemotherapy extremely challenging. The currently poor outcomes of glioblastoma emphasize the urgent need for better understanding of its molecular mechanisms and identification of novel therapeutic targets for this lethal disease.

Molecular studies have shown remarkable genomic heterogeneity of glioblastoma and the

existence of molecular subclasses within glioblastoma that may be potentially applied to stratification of treatment [3], and these studies have identified several important genomic abnormalities in glioblastomas including dysregulation of growth factor signaling via amplification and mutational activation of receptor tyrosine kinase (RTK) genes; activation of the phosphatidylinositol-3-OH kinase (PI3K) pathway; and inactivation of the P53 and retinoblastoma (Rb) tumor suppressor pathways [4]. The frequently mutated genes in glioblastoma include NF1, P53, Rb, PTEN, EGFR, ERBB2, PIK-3R1, PIK3CA, and IDH1/2 etc [4, 5]. In addition, studies have also indicated that epigenetic alterations such as DNA hypermethylation of MGMT and p16 promoters are also involved in glioblastoma [4, 6].

Liver kinase B1 (LKB1) is a serine/threonine kinase (also named STK11) that activates adenosine monophosphate-activated protein kinase (AMPK) and 12 other kinases involved in cellular development, cell polarity, metabolism, growth, and apoptosis [7]. LKB1 was first recognized as a tumor suppressor from germ-line mutations in Peutz-Jeghers syndrome (PJS), which is characterized by gastrointestinal hamartomas and increased risk of cancer [8]. Inactivating mutations in LKB1 have been found in sporadic lung adenocarcinoma, cervical, breast, pancreatic, and cholangiocarcinoma cancers [9-12]. LKB1 is thought to suppress tumor by negatively regulating tuberous sclerosis complex (TSC1/2) on mammalian target of rapamycin (mTOR) signaling via the central metabolic switch, AMP-activated protein kinase (AMPK) [7]. Inactivation of LKB1 has been shown to have significant impact on cancer malignancy. For example, a previous study showed that LKB1 deficiency can significantly enhance carcinogenic effect of P53 or PTEN inactivation and KRAS activation in mouse model [13-15]. Most recently, a study clinically found that LKB1 loss can serve as a predictive biomarker for aggressive KRAS-mutant lung adenocarcinoma [16].

Focal adhesion kinase (FAK) acts as a signaling node at cell adhesion sites to promote cytoskeletal reorganization, adhesion, and migration [17]. FAK also works in unison with LKB1 to regulate cell motility through integrins and growth factor receptors by relaying cues from the extracellular matrix (ECM) through the plasma membrane, and into the cytoplasm [18]. A recent study demonstrated that LKB1 expression was significantly decreased in glioma tissues, and was significantly associated with malignancy and patient survival [19]. While the mechanistic relevance and clinical significance of LKB1 loss in brain cancer remain unclear.

In this study, we reported an identification of LKB1 deletion in a case of glioblastoma by whole genome sequence analysis, and decrease, loss of LKB1 protein in a cohort of human glioblastoma by immunohistochemistry analysis. We further investigated the effect of LKB1 knockdown via small interfering RNA (siRNA) on *in vitro* cellular proliferation, adhesion, and invasion using U87 and T98 glioblastoma cell lines. Moreover, we identified potential target genes and critical signaling pathways involving LKB1 loss in glioblastoma and assessed their therapeutic implications. We demonstrated that downregulation of LKB1 may contribute to the pathogenesis and malignancy of glioblastoma and may have important clinical implications for stratification and treatment of glioblastoma patients.

Material and methods

Patients and clinical data collection

All human cases of glioblastoma derived from 58 patients, diagnosed with histologically verified glioblastoma at City of Hope National Medical Center or Taipei Medical University. This study was conducted with the approval of the ethics committee of City of Hope National Medical Center and Taipei Medical University. All specimens were formaldehyde fixed-paraffin embedded (FFPE) tissues.

Fluorescence in situ hybridization (FISH) and immunohistochemistry (IHC) analysis

FISH and IHC assays of LKB1 were done on FFPE slides from human tissues according to methods previously reported [12]. Antibodies against LKB1 (ab58786), P53, PTEN, Vinculin, and rabbit polyclonal against Talin1, FAK1, phospho-FAK, total and phospho-S6k (Thr389), total and phosph-4E-BP (Thr37/46), AMPK, phospho-AMPK (Thr172), and cleaved PARP (Asp-214) were obtained from Abcam, Sigma, Santa Cruz Biotechnology, Inc. (Santa Cruz, CA) and

Cell Signaling Technology (Beverly, MA). Rabbit polyclonal anti-LKB1 antibody (ab58786, Abcam) (1:200 dilutions) was applied for IHC staining. Cytoplasmic and nuclear LKB1 immunoreactivity was assessed. The staining was graded based on intensity of general IHC staining and percentage of positive staining as negative (-) (< 5% tumor cells positive, weak), (+) (5%-24% tumor cells positive, moderate), and (++) (> 25% tumor cells positive, strong) [20].

LKB1 siRNA transfection, migration, and matrigel invasion assays

LKB1 siRNA (human) and scramble siRNA were purchased from Santa Cruz Biotechnology, Inc. (Santa Cruz, CA). For knockdown assays, 1×10^5 glioblastoma cells (U87 and T98) were seeded on 6-well plates and transfected with 4.5 µl control or LKB1 gene-specific siRNA (10 µM) and 4.5 µl Lipofectamine RNAiMAX (Invitrogen) complex. Cell proliferation was determined by cell proliferation assay MTS kit (Promega, Madison WI, USA). Migration and invasion assays were performed as described in previous report [21]. Three sets of the same experimental conditions were performed.

Cell-adhesion assay to extracellular matrix

Adhesion of cells to ECM was assayed by using 24-well plates coated with 20 µg/ml fibronectin, laminin, collagen IV or bovine serum albumin (BSA)-control substrate (Millipore Corporation) at 4°C overnight. 72 hours after transfection with either control or LKB1 siRNA, T98 and U87 cells (2.5×10^5) were incubated for 1.5 hours at 37°C and 5% CO_2, washed in PBS, stained with 0.2% crystal violet (Sigma-Aldrich) in 10% ethanol for 5 minutes at room temperature, and rinsed again in PBS. Stained cells were later counted in a number of random fields under 40× magnification. Results from three independent experiments with triplicate repeats per experiment were pooled.

Illumina Genome Analyzer (Solexa) whole-genome sequencing and RNA sequencing analysis

Genomic DNA from patient saliva was isolated and analyzed in accordance with methods from Oragene DNA (DNA Genotek Inc.) for germline DNA sequencing. DNA extraction of FFPE tissue, library preparation and whole-genome sequencing (Illumina Genome Analyzer IIx) and data analysis were performed and analyzed, according to methods previously reported [22]. At 72 hours post-transfection of siRNA, total RNA was extracted for RNA sequencing analysis. Transcriptome libraries were constructed and sequenced (Illumina Hiseq 2500), and RNA-seq data analysis was performed as we previously described [20, 23]. Gene set enrichment analysis (GSEA) was applied to examine pathways significantly modulated upon LKB1 knockdown [24].

The pcDNA3-Flag PTEN plasmid (Addgene plasmid # 78777 [25] or control pcDNA3 plasmid (4.5 µg) with control or LKB1 siRNA (4.5 µl) was transfected into T98 cells seeded in 6 well-plates using Lipofectamin 2000 reagent. At 72 hours post-transfection, cell numbers were counted, and Flag-PTEN expression was measured by Western blot using anti-FLAG antibodies (Flag M2 antibody, Sigma, Saint Louis, MO).

Metformin treatment and apoptosis assay

U87 and T98 cells were transfected with either control siRNA or LKB1 siRNA. At 24 hours post-transfection, cells were treated for 72 hours with 25 mM metformin. Metformin-induced apoptosis in these cells was measured by flow cytometry (Alexa Fluor 488-labeled Annexin-V and propidium iodide staining) in accordance to the manufacturer's protocol. Total proteins were also extracted for Western blot analysis.

Correlation of LKB1 mRNA expression with GBM survival based on publicly available TCGA gene expression data

To measure the relevance and importance of LKB1 in human glioblastoma, the normalized mRNA expression levels of LKB1 (level 3 data, Affymetrix Human Exon 1.0 ST) in 348 cases of human glioblastoma tissues were obtained from the Cancer Genome Atlas (TCGA) public data portal (https://tcga-data.nci.nih.gov/tcga/), as we described previously [20, 26]. The clinical information for each patient was also downloaded. To correlate survival, gene expression ≤ 33rd percentile was considered low, ≥ 67th percentile was considered high, and those falling within the 33rd and 67th percentile were considered medium. Kaplan-Meier survival analysis was used to estimate the association

of the Lkb1 gene's expression with the survival of glioblastoma patients. The survival package in R (R Foundation for Statistical computing) was used for statistical analyses.

Data management and statistical analysis

Averaged values of cell proliferation, adhesion, transwell migration, invasion, and apoptosis experiments were used to generate bar graphs depicting average values ± standard deviations. Group comparisons for continuous data were conducted using Student's *t* tests or x^2 test. Statistical significance was set at $P < 0.05$.

Results

Identification of LKB1 downregulation in glioblastoma

We adopted whole-genome sequencing to characterize genomic abnormalities in a glioblastoma tissue. Whole genome sequencing analysis showed a copy number decrease of ~4.2-Mb DNA region at chr19p13.3. This DNA region contained multiple genes, including tumor suppressor LKB1 gene (**Figure 1A**). FISH analysis revealed heterozygous loss of LKB1 expression showing as single or double deletion signal (red signal) of LKB1 (Figure S1A). Quantitative analysis showed that 104 out of 200 (57%) cells lost one allele of LKB1, and 52 out of 200 (26%) lost two alleles of LKB1. DNA Sequencing and PCR analysis revealed somatic biallelic deletion of Exon 3 in LKB1 glioblastoma tissue compared to saliva (Figure S1B), indicating complete loss of LKB1 tumor suppressor in the glioblastoma tissue. IHC further demonstrated that the majority of cancer cells in the glioblastoma tissue were negative for LKB1 immunostaining (**Figure 1B**). We further investigated LKB1 expression in 58 cases of glioblastoma by IHC analysis. Complete loss of LKB1 immunostaining was found in 8.6% (5/58) glioblastoma tissues, while decrease of LKB1 immunostaining was found in 29.3% (17/58) of glioblastoma tissues (**Figure 1C**). All other cases had a moderate to strong immunostaining for LKB1 (**Figure 1D**). Interestingly, we also observed that LKB1 immunostaining was much lower in high-grade undifferentiated gliomas compared to low-grade gliomas like astrocytoma (Figure S2); suggesting LKB1 deficiency may be potentially associated with gliomas differentiation.

We next analyzed the correlation of LKB1 mRNA level with the overall survival of glioblastoma patients using TCGA data of glioblastoma. The mRNA expression of LKB1 in these patients was categorized into three quartiles based on low (N = 116, blue line), medium (N = 116, green line) and high (N = 116, red line) expressions (**Figure 1F**). The lower LKB1 expression was associated with shorter overall survival compared with high expression in glioblastoma patients ($P = 0.0032$). For these patients with lower LKB1 level, the overall survival probability was about 73% and 44% at 36 and 60 months, respectively, and those with higher LKB1 levels showed a better survival probability of 82% and 78% at 36 and 60 months, respectively.

Impact of knockdown of LKB1 on mTOR pathway, proliferation, and its interaction with PTEN

To examine the impact of LKB1 on malignancy of glioblastoma cells, we knocked down LKB1 in two LKB1-competent glioblastoma cell lines: U87 (harboring mutant P53 and inactivated PTEN) and T98 (harboring wild-type P53 and inactivated PTEN). We found knockdown of LKB1 drastically decreased phosphorylated AMPK and increased in phosphorylated S6K and 4E-BP1 (downstream targets of mTOR signaling pathway) in both U87 cells (**Figure 2A**, left panel) and T98 cells (**Figure 2A**, right panel), indicating over-activation mTOR signaling pathway upon LKB1 knockdown. In addition, Western blot analysis revealed a moderate to strong increase of phosphorylated AKT and ERK in both cell lines. Consistent with activation of these pathways, LKB1 knockdown resulted in a significant increase of *in vitro* proliferation in both U87 cells (**Figure 2B**, upper panel) and T98 cells (**Figure 2B**, lower panel) at 72 hours post-transfection of LKB1 siRNA. Therefore, these data strongly suggest knockdown of LKB1 enhances the malignancy of glioblastoma via enhanced cell proliferation and anti-apoptotic signaling pathways.

LKB1 and PTEN are two tumor suppressors that regulate the mTOR signaling pathway. LKB1 is shown to interact with and phosphorylate PTEN, and loss of this interaction might contribute to PJS [27]. Since PTEN is frequently

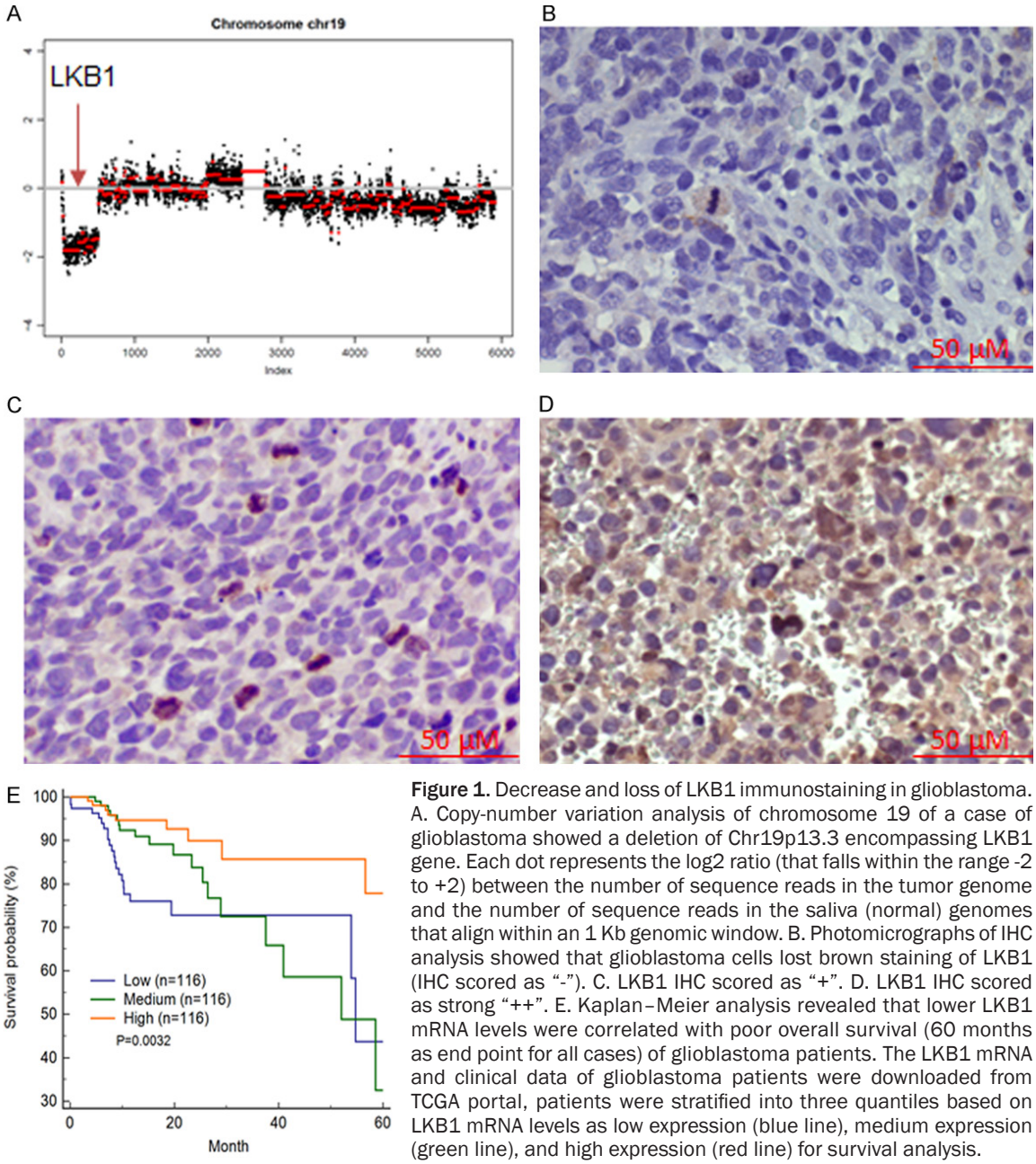

Figure 1. Decrease and loss of LKB1 immunostaining in glioblastoma. A. Copy-number variation analysis of chromosome 19 of a case of glioblastoma showed a deletion of Chr19p13.3 encompassing LKB1 gene. Each dot represents the log2 ratio (that falls within the range -2 to +2) between the number of sequence reads in the tumor genome and the number of sequence reads in the saliva (normal) genomes that align within an 1 Kb genomic window. B. Photomicrographs of IHC analysis showed that glioblastoma cells lost brown staining of LKB1 (IHC scored as "-"). C. LKB1 IHC scored as "+". D. LKB1 IHC scored as strong "++". E. Kaplan–Meier analysis revealed that lower LKB1 mRNA levels were correlated with poor overall survival (60 months as end point for all cases) of glioblastoma patients. The LKB1 mRNA and clinical data of glioblastoma patients were downloaded from TCGA portal, patients were stratified into three quantiles based on LKB1 mRNA levels as low expression (blue line), medium expression (green line), and high expression (red line) for survival analysis.

inactivated in glioblastoma, to investigate the impact of PTEN status on the enhanced proliferation by LKB1 knockdown, wild-type PTEN is reconstituted into T98 cells (harboring an inactivated PTEN). T98 cells were simultaneously transfected with both LKB1 siRNA (or control siRNA) and wild-type PTEN plasmid (or control plasmid), and at 72 h post-transfection, mTOR activation that is reflected by phosphorylated S6K level and cell proliferation were measured. As shown in **Figure 2C**, reconstitution of wild-type PTEN (Flag-tagged) moderately decreased but didn't completely abolish the enhanced activation of mTOR signaling pathway upon LKB1 knockdown. And in consistent with mTOR activation, reconstitution of wild-type PTEN moderately suppressed *in vitro* cellular proliferation, and partially abolished the elevated proliferation caused by LKB1 knockdown in T98 cells (**Figure 2D**), which indicates LKB1 and PTEN may synergize to suppress mTOR-mediated cell proliferation in glioblastoma, and LKB1 loss enhances cell proliferation in glioblastoma cells with wild-type PTEN.

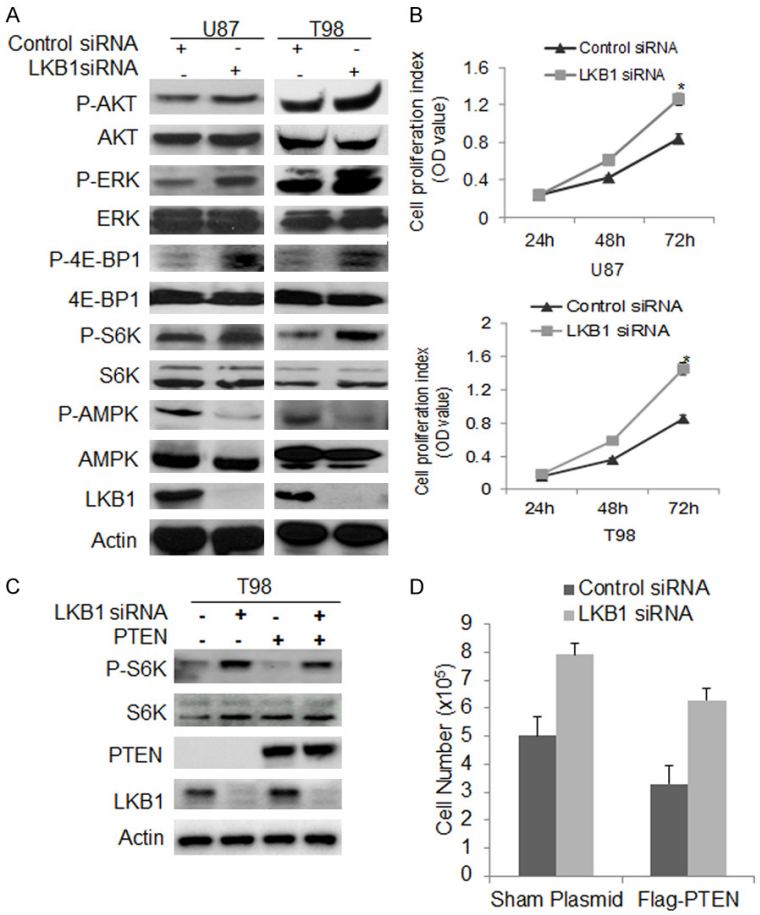

Figure 2. Impact of LKB1 knockdown on mTOR pathway, proliferation, and its interaction with PTEN in glioblastoma cells. A. Western blot analysis of cell lysates of U87 and T98 cells transfected with either LKB1 siRNA or scramble siRNA harvested at 72 h post transfection. Actin serves as loading control, and total and phosphorylated (P-) AMPK, 4E-BP1, and S6K and ERK and AKT were detected with the appropriate antibodies. B. A histogram of 72 h proliferation shows knockdown of LKB1 significantly increased the *in vitro* proliferation of both U87 (mutated P53, upper panel) and T98 cells (wild-type P53, lower panel) (*$P < 0.05$, compared with control cell transfected with control siRNA). C. Western blot of reconstituted wild-type PTEN (Flag-tagged) and phosphorylated S6K (P-S6K) in LKB1-attenuated T98 cells. D. Cell numbers of LKB1-attenuated T98 cells after reconstitution of wild-type PTEN. ($P < 0.05$), Sham plasmid was used as a control for PTEN plasmid. Cells were co-transfected with both LKB1 (control) siRNA and wild-type PTEN (sham) plasmid, at 72 h post-transfection, cells were counted and lysates were collected for Western blot analysis.

Impact of knockdown of LKB1 on adhesion, and invasion in glioblastoma cells

In consistent with its important role in cellular polarity [28], we herein found that knockdown of LKB1 induced dramatic morphological changes from tightly clustered cobblestone morphology to a loose elongated appearance in both U87 cells (**Figure 3A**, left panel) and T98 cells (**Figure 3A**, right panel). We further found that knockdown of LKB1 significantly enhanced adhesion of T98 cells to ECM components including laminin, collagen IV, and especially fibronectin (**Figures 3B**, S3, $P < 0.05$). Same results were also observed in U87 cells (data not shown). Furthermore, using migration and matrigel invasive chamber assays, we identified that knockdown of LKB1 significantly enhanced the migration (**Figures 3C**, S4, $P < 0.05$) and invasive potentials (**Figures 3D**, S5, $P < 0.05$) of both U87 and T98 cells.

Enriched gene sets in glioblastoma upon LKB1 knockdown

To determine the effects of LKB1 knockdown on the gene expression in glioblastoma, we combined siRNA knockdown, RNAseq, and quantitative pathway analysis to elucidate gene sets and signal pathways affected by LKB1 knockdown in both U87 and T98 glioblastoma cells. Cluster heat maps of differential gene expression upon LKB1 knockdown are shown in **Figure 4A**. RNA sequencing analysis revealed 238 genes were differentially expressed in these two glioblastoma cells compared to control cells (Table S1). RNAseq data has been submitted to GEO with access number GSE91016. RNA-seq analysis identified a variety of genes related to cell morphology, cell adhesion, and migration were significantly up-regulated in these two glioblastoma cells upon LKB1 knockdown. Differential gene expression of LKB1, Vinculin (VCL), Talin 1 (Talin/TLN), CLDN12, HMMR, CCDC99, TTL, TNC, and VCAN were confirmed by qRT-PCR (**Figure 4B**), and some by Western blot analysis (**Figure 4C**).

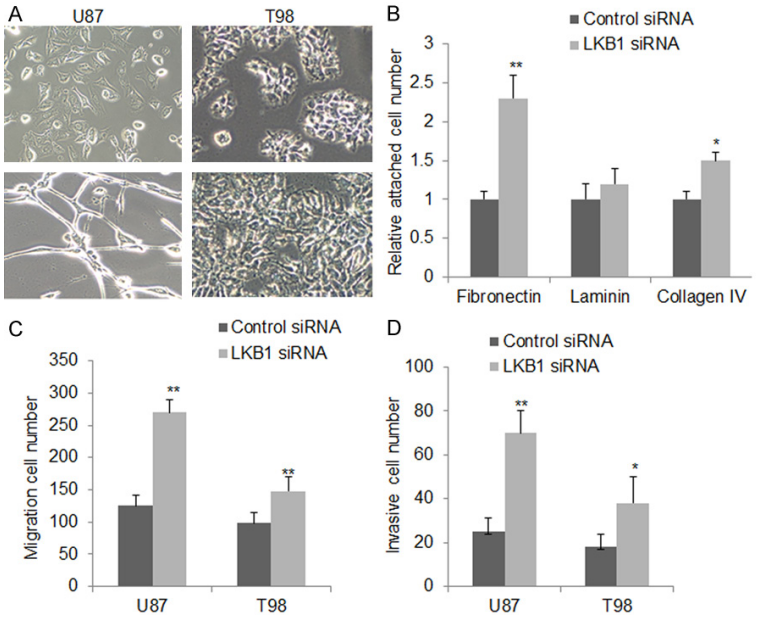

Figure 3. Impact of LKB1 knockdown on adhesion, and invasion in glioblastoma cells. A. Morphological change of U87 (left panel) and T98 (right panel) glioblastoma cells upon LKB1 knockdown. B. Increased adhesion to extracellular matrix components of fibronection, laminin, and collagen IV in two glioblastoma cells upon LKB1 knockdown. C. Quantitative analysis of migrated cells of the migration chamber at the times indicated in control or LKB1 siRNA-transfected U87 and T98 glioblastoma cell lines (N = 3 replicates per cell type). Error bars show SD (*P < 0.05, compared with control siRNA). D. Quantitative analysis of invading cells of matrigel transwell membranes seeded with U87 and T98 glioblastoma cell lines previously transfected with indicated siRNAs, 24 h after incubation. Data are shown as mean values graphed for indicated cells on the right (N = 3 replicates per cell type). Error bars show SD (*P < 0.05, **P < 0.01, compared with control siRNA).

Using GSEA and Kyoto Encyclopedia of Genes and Genomes (KEGG) [24], we identified multiple gene sets that were significantly enriched in LKB1-attenuated glioblastoma cells (P < 0.05). The top enriched gene sets were FAK, ECM receptor interaction, cellular motility, and vasculature development (**Figure 4D**). These signaling pathways may be potentially involved in the enhanced malignancy via LKB1 inactivation in glioblastoma.

Knockdown of LKB1 enhanced FAK signaling pathways in glioblastoma cells

RNA sequencing analysis revealed that mRNA expressions in 87 out of 181 genes in the FAK signaling pathway were significantly affected upon knockdown of LKB1 in glioblastoma cells. We then further investigated the interaction between cytoskeletal proteins and FAK signaling pathway in glioblastoma cells upon knockdown of LKB1. GSEA indicated that FAK pathway is significantly enriched in both U87 (**Figure 5A**, upper panel) and T98 glioblastoma cells (**Figure 5A**, lower panel) upon LKB1 knockdown. Consistently, Western blot analysis confirmed that knockdown of LKB1 dramatically upregulated phosphorylated FAK at Tyrosine 387 in both U87 and T98 glioblastoma cells. A previous study revealed that Src is activated in LKB1-deficient primary and metastatic lung cancer [29]. In our study, overactivation of Src was not observed in LKB1-attenuated glioblastoma cells (**Figure 5B**). Since Talin is an upstream molecule of focal adhesion proteins involved in activating integrin and FAK signaling pathways [30], we then investigated what role the cytoskeletal proteins Talin and Vinculin contribute to overactivation of FAK signaling pathway upon LKB1 knockdown. To address this question, we simultaneously knocked Talin and LKB1 in glioblastoma cells to compare FAK activation. Western blot analysis showed that knockdown of Talin significantly attenuated overactivation of FAK induced by LKB1 knockdown in both U87 (**Figure 5C**) and T98 glioblastoma cells (**Figure 5D**). Taken together, these results indicate that activated FAK signaling pathways by LKB1 knockdown may be mediated by changes in the expression of cytoskeleton proteins such as Talin.

Therapeutic implications of targeting mTOR and FAK in glioblastoma cells upon LKB1 downregulation

Since LKB1 knockdown dramatically enhanced activation of both mTOR and FAK signaling pathways, we investigated the potential therapeutic implications of targeting these signaling pathways upon LKB1 downregulation. Rapamycin (100 nM) and PF-573288 (2 μM) were used as mTOR and FAK pathway inhibitor, respectively. As shown in **Figure 6A**, mTOR inhibitor rapamycin dramatically decreased phos-

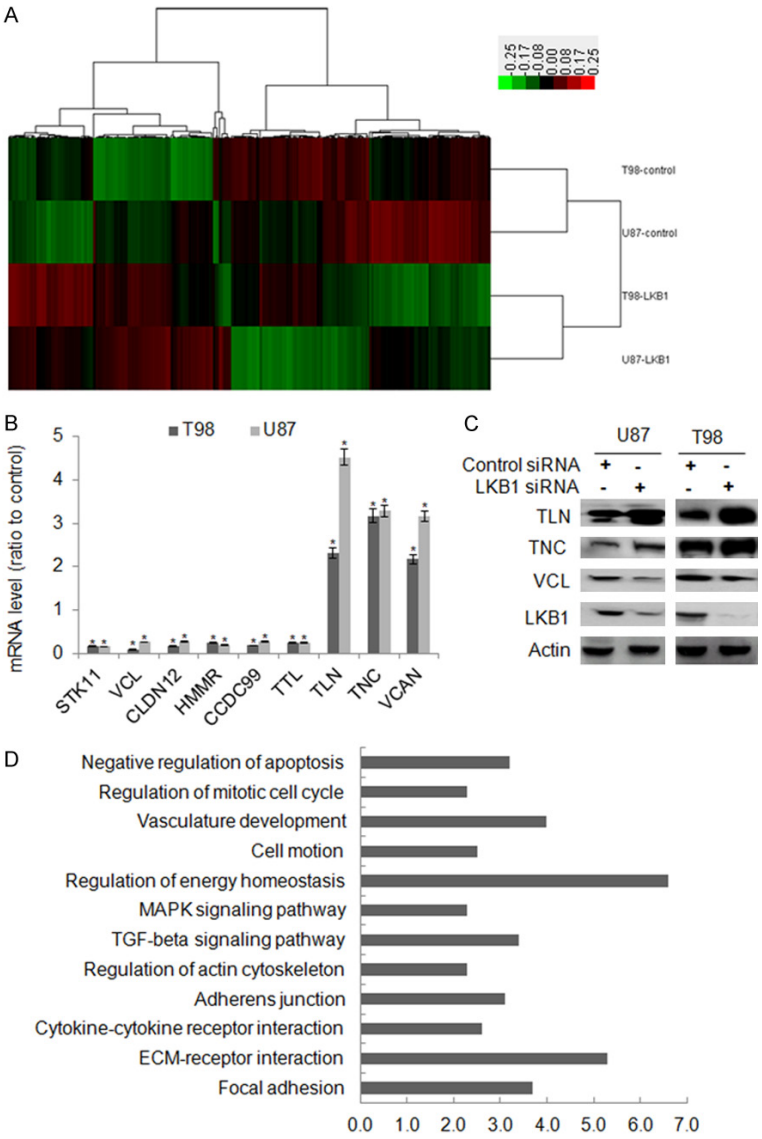

Figure 4. Identification of genes and signaling pathways of LKB1-attenuated glioblastoma cells by RNAseq and gene set enrichment analysis. (A) Unsupervised hierarchical clustering analysis of differentially expressed genes in glioblastoma U87 and T98 cell lines upon LKB1 knockdown (LKB1 for LKB1 siRNA, and Control for control siRNA). Genes are represented in rows (red for significant enrichment of overexpressed genes; green for significant enrichment of downregulated genes; FDR < 0.05, $P < 0.05$). Differentially expressed candidate genes were validated by (B). qRT-PCR analysis (*$P < 0.05$, compared with control siRNA) and (C) Western-blot analysis. Data of qRT-PCR are presented as ratio of cells transfected with LKB1 siRNA to these cells transfected with control siRNA. (D) The list of gene sets enriched by knockdown of LKB1 in both T98 and U87 glioblastoma cell lines ($P < 0.05$).

phorylated S6K (one of mTOR downstream target proteins) in both control and LKB1-attenuated T98 cells, indicating suppression on mTOR pathway. While FAK inhibitor PF-573288 significantly suppressed activation of FAK signaling pathway showing as decreased phosphorylated FAK (Tyrosine 387) in T98 cells upon LKB1 knockdown (**Figure 6B**). Notably, rapamycin significantly inhibited LKB1-enhanced cell proliferation, it did not decrease cell invasion (**Figure 6C**). While FAK inhibitor significantly decreased cell invasion, but had little effect on cellular proliferation (**Figure 6D**) in LKB1-attenuated T98 cells, indicating a combination of mTOR and FAK inhibitors may suppress both proliferation and invasion enhanced by LKB1 loss. In addition, both mTOR and FAK inhibitors do not alter the differentially expressed cytoskeletal proteins Talin and vinculin by LKB1 knockdown (**Figure 6A** and **6B**), further suggesting that cytoskeletal protein changes might be independent of mTOR activation and likely upstream of FAK signaling pathway.

Impact of LKB1 knockdown on sensitivity of glioblastoma cells to metabolic stress

To investigate the impact of LKB1 on sensitivity of U87 and T98 to metformin, LKB1 was first knocked down by siRNA transfection; and at 24 hours post-transfection, cells were treated with 25 mM metformin for 72 hours, and then cells were collected for apoptosis analysis. Western blot analysis showed that LKB1 was dramatically decreased in both U87 and T98 (**Figure 7A** and **7B**), and knockdown of LKB1 decreased p-AMPK. Metformin strongly activated p-AMPK in control U87 and T98 cells transfected with control siRNA, but not in LKB1-attenuated glioblastoma cells. Compared to control, metformin induced a strong apoptotic response in LKB1-attenuated cells, being shown as increase in the apoptosis biomarker cleaved PARP in

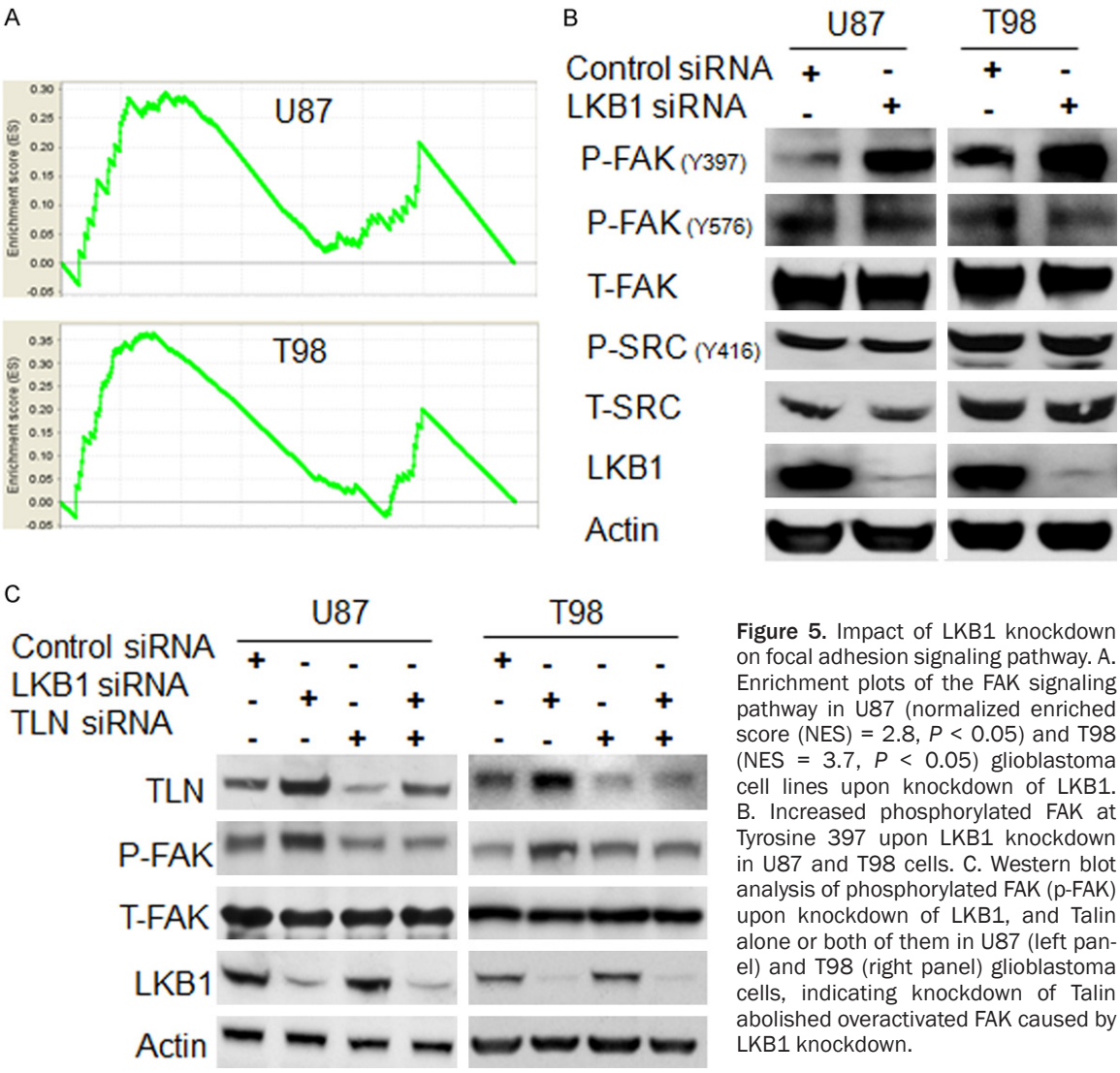

Figure 5. Impact of LKB1 knockdown on focal adhesion signaling pathway. A. Enrichment plots of the FAK signaling pathway in U87 (normalized enriched score (NES) = 2.8, $P < 0.05$) and T98 (NES = 3.7, $P < 0.05$) glioblastoma cell lines upon knockdown of LKB1. B. Increased phosphorylated FAK at Tyrosine 397 upon LKB1 knockdown in U87 and T98 cells. C. Western blot analysis of phosphorylated FAK (p-FAK) upon knockdown of LKB1, and Talin alone or both of them in U87 (left panel) and T98 (right panel) glioblastoma cells, indicating knockdown of Talin abolished overactivated FAK caused by LKB1 knockdown.

both U87 and T98 glioblastoma cells (**Figure 7A** and **7B**). Quantitative analysis of apoptotic cells by Annexin-V apoptosis assay showed that LKB1 knockdown significantly increased metformin-induced apoptosis in both U87 (**Figure 7C**) and T98 (**Figure 7D**) cells, independent of their P53 status. Therefore, the above findings suggest that deficiency of the LKB1-AMPK signaling pathway may sensitize glioblastoma cells to metformin treatment.

Discussion

Molecular characterization of cancer genome can help identify novel genetic alternations and lead to development of prognostic biomarkers and personalized therapies. In this study, we conducted whole-genome sequencing of a case of glioblastoma with rare pathological features of epithelial differentiation and biphasic architectures. Inactivation of the P53 is a well-known genetic abnormality in various human cancers [31]. Of interest, our sequencing analysis also found a somatic, homozygous P53 missense mutation C833T P278L in exon-8 DNA binding domain (Figure S6A). IHC analysis showed that P53 protein is strongly positive in all cancer cells except normal endothelial cells (Figure S6B). Importantly, we also identified loss of LKB1 tumor suppressor in this glioblastoma, which is rarely reported. Therefore, we further investigated LKB1 in a cohort of glioblastoma patients and found a moderate frequency of decrease and loss of LKB1 immunostaining in glioblastoma tissues, although the underlying causes for decrease and loss of

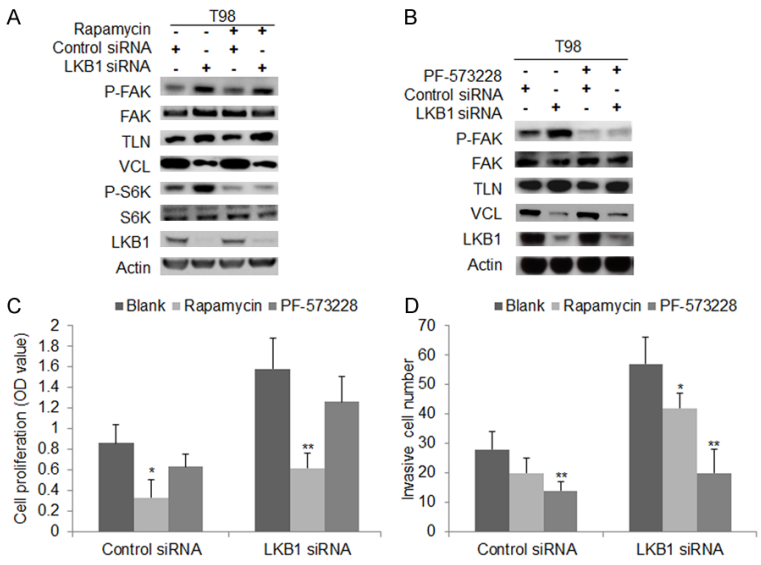

Figure 6. Impact of targeting mTOR and FAK on enhanced cell proliferation and invasion upon LKB1 knockdown. (A) Western blot analysis of Talin, vinculin, phosphorylated S6K, phosphorylated FAK in LKB1-attenuated T98 cells treated with rapamycin (mTOR inhibitor). (B) Western blot analysis of P-FAK, TLN and VCL in LKB1-attenuated T98 cells treated with FAK inhibitor PF-573228. Impact of rapamycin and PF-573228 on enhanced (C). cellular proliferation, and (D). invasion in LKB1-attenuated T98 cells. At 24 h post-transfection of control or LKB1 siRNA, T98 cells were further treated with mTOR or FAK inhibitor for 72 hours for Western blot, cell proliferation, and invasion analysis (**P* < 0.05, ***P* < 0.01, compared to untreated blank).

LKB1 immunostaining remain to be further addressed. Inactivation of LKB1 has been shown to have significant impact on cancer malignancy and patient prognosis [13-16]. Several studies also demonstrated that inactivation of LKB1 can significantly enhance metastasis of lung adenocarcinomas and melanoma driven by KRAS oncogene [32, 33]. These studies indicate LKB1 loss can dramatically enhance the malignancy caused by other genetic abnormalities. Consistently, a recent study demonstrated that downregulation of LKB1 was significantly associated with malignancy and survival of glioma patients [19].

To reveal molecules and signaling pathways upon LKB1 decrease and loss in glioblastoma, using RNAseq analysis, we identified that cellular adhesive and cytoskeletal proteins Talin, vinculin, CLDN12, HMMR, CCDC99, TTL, TNC, and VCAN were differentially expressed at transcriptional level upon LKB1 knockdown in two glioblastoma cells. Functionally, these proteins play critical roles in focal adhesion, cellular migration and metastasis of cancers. For example, overexpression of Talin, a cytoskeletal protein, is directly correlated with invasion and metastasis of human oral squamous cell carcinoma [34]. Vinculin, an adhesion protein that was reported to participate in cell to cell adhesions in metastatic human squamous cell carcinoma [35], was also found to be significantly downregulated in glioblastoma cells upon LKB1 knockdown. In agreement with changes of cytoskeletal protein expression, we observed a pronounced elevated activation of FAK signaling pathway upon knockdown of LKB1 in glioblastoma cells. Studies have demonstrated that LKB1 deficiency plays a critical role in cell polarity and migration of neural progenitor cells *in vivo* [36]. In cancer, FAK has been found to be critical for cell adhesion and invasion through acting as a signaling node at focal contacts to promote cytoskeletal reorganization, adhesion, migration, and survival [17]. These previous reports and our findings consistently show that LKB1 is involved in cell migration. A study revealed overactivated SRC in LKB1-deficient primary and metastatic lung cancer induced abnormal FAK signaling in animal model [29]. Our study revealed activation of FAK, not activation of SCR, occurred upon LKB1 knockdown in glioblastoma, suggesting variable mechanisms exist. Based on our data, we conclude that activation of FAK signaling is likely mediated by changes in cytoskeletal protein expression, organization, and interaction with integrin signaling pathway.

Inactivation of LKB1 has been shown to have significant impact on how cancer cells respond to different stresses. Rapamycin has recently been identified as a cytostatic agent with significant activity in various human cancer cell lines and tumor models [37]. Based on this data, phase I, II, and III trials are being conducted for evaluation of rapamycin and its derivatives in a variety of cancers including glioblastomas [37, 38]. We have herein shown that loss

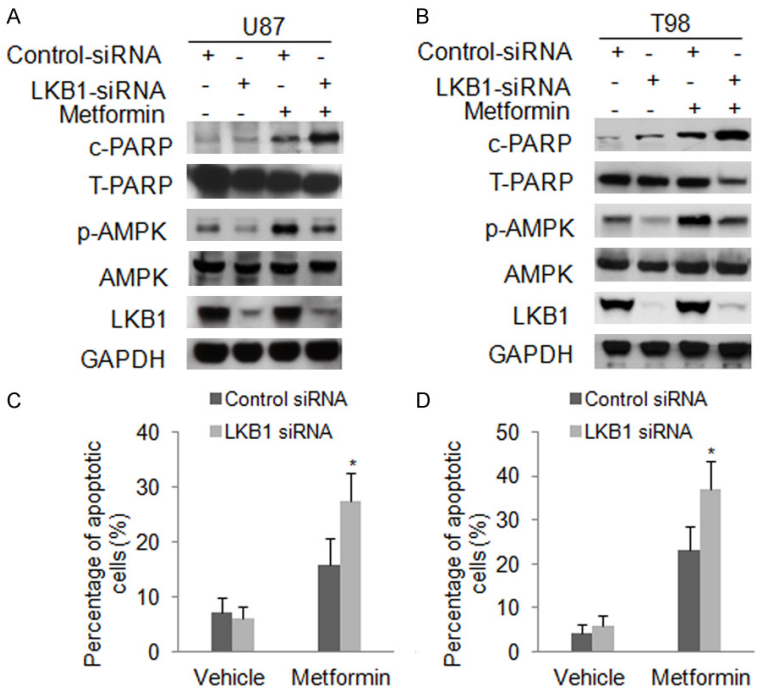

Figure 7. Impact of LKB1 knockdown on sensitivity of U87 and T98 cells to metformin treatment. Western blot showed that LKB1 knockdown resulted in a decrease of metformin-induced p-AMPK and cleaved PARP (c-PARP) in (A). U87 and (B). T98 cells. Quantitative flow cytometry analysis demonstrated that LKB1 knockdown enhanced metformin-induced apoptosis in (C). U87 and (D). T98 cells. Cells were transfected with control or LKB1 siRNA, 24 hs later, cells were further treated with 25 mM metformin for additional 72 h, and apoptotic cells were analyzed (*P < 0.05 compared with cells transfected with control siRNA).

of LKB1 overactivates mTOR signaling pathway and promotes cellular proliferation in glioblastoma cells. Interestingly, we have further demonstrated that rapamycin can significantly suppress enhanced cellular proliferation by LKB1 knockdown. Several studies observed that LKB1-deficient non-small cell lung cancers (NSCLC) displayed selective response to mitochondrial inhibitor phenformin as a single agent [39]. Additionally, LKB1 and PTEN are two tumor suppressors that suppress the mTOR signaling pathway. And deletion of LKB1 and PTEN was found to synergize in carcinogenesis of mouse bladder, ovarian, and endometrial cancers [40-42]. In agreement with the above observations, we herein found that reconstitution of wild-type PTEN only partially abolished the enhanced mTOR signaling pathway and cell proliferation caused by LKB1 loss. Stimuli that normally activate LKB1-AMPK fail to result in decreased mTOR activity in LKB1-null cells and can activate apoptosis [39]. Similarly, another study demonstrated that metabolic drugs like mitochondrial inhibitors metformin and its analog phenformin selectively induce apoptosis in LKB1-deficient NSCLC cells [43]. Herein, we have shown that LKB1-attenuated glioblastoma cells are more sensitive to metformin. Interestingly, Carmignani et. al. report that metformin and arsenic trioxide can induce apoptosis in glioblastoma stem cells, which suggests metformin can cross the blood brain barrier and be a potential anticancer agent for glioblastoma [44]. A study revealed that the combined inhibition of SRC, PI3K, and MEK1/2 resulted in synergistic tumor regression [29], and the combined inhibition of SRC, PI3K, and MEK1/2 resulted in synergistic tumor regression. Herein, we have demonstrated mTOR and FAK inhibitor may potentially be used for glioblastoma treatment to suppress rapid proliferation and invasion. In view of the invasive nature of glioblastoma and limited therapies currently available, there is a great need to stratify all brain cancers according to their molecular characteristics and treat them with targeted therapeutic approaches. Identification of LKB1 status may potentially represent a unique opportunity to classify brain cancer and holds significant diagnostic and therapeutic implications for future studies.

In summary, the study showed that LKB1 downregulation significantly enhances malignant characteristics including proliferation and invasion through enhancing FAK, mTOR pathways in glioblastoma cells. The study further demonstrated therapeutic significance of targeting mTOR, metabolic response, and FAK pathways in LKB1-attenuated glioblastoma cells. These findings indicate LKB1 downregulation may contribute to malignancy and prognosis of glioblastoma, and may have potential therapeutic implications for LKB1-deficient glioblastoma patients.

Acknowledgements

We thank Victoria Bedell at the City of Hope Cytogenetic Core for assistance in LKB1 FISH assay, and Sofia Loera at the City of Hope pathology Core for IHC staining, Brown Lucy at the City of Hope flow cytometry Core for apoptosis analysis. We thank Dr. Rajendra Pangeni for assistance in TCGA data analysis. The study was supported in part by the "TMU Research Center of Cancer Translational Medicine" from The Featured Areas Research Center Program within the framework of the Higher Education Sprout Project by the Ministry of Education (MOE) in Taiwan, health and welfare surcharge of tobacco products grant MOHW107-TDU-B-212-114020, MOHW107-TDU-B-212-114014 and MOHW107-TDU-B-212-114026B; and Ministry of Science and Technology grant MOST 106-3114-B-038-001, MOST 107-2321-B-038-002, MOST 108-2321-B-038-003.

Disclosure of conflict of interest

None.

Address correspondence to: Dr. Keqiang Zhang, Department of Surgery, City of Hope National Medical Center, Duarte, CA, USA. Tel: (626) 235-3489; E-mail: kzhang@coh.org; Dr. Yun Yen, Program of Cancer Biology and Drug Discovery, College of Medical Science and Technology, Taipei Medical University, Taipei, Taiwan. Tel: (886) 970-405-888; E-mail: yyen@tmu.edu.tw

References

[1] Stupp R, Hegi ME, Mason WP, van den Bent MJ, Taphoorn MJ, Janzer RC, Ludwin SK, Allgeier A, Fisher B, Belanger K, Hau P, Brandes AA, Gijtenbeek J, Marosi C, Vecht CJ, Mokhtari K, Wesseling P, Villa S, Eisenhauer E, Gorlia T, Weller M, Lacombe D, Cairncross JG, Mirimanoff RO; European Organisation for Research and Treatment of Cancer Brain Tumour and Radiation Oncology Groups; National Cancer Institute of Canada Clinical Trials Group. Effects of radiotherapy with concomitant and adjuvant temozolomide versus radiotherapy alone on survival in glioblastoma in a randomised phase III study: 5-year analysis of the EORTC-NCIC trial. Lancet Oncol 2009; 10: 459-66.

[2] Furnari FB, Fenton T, Bachoo RM, Mukasa A, Stommel JM, Stegh A, Hahn WC, Ligon KL, Louis DN, Brennan C, Chin L, DePinho RA, Cavenee WK. Malignant astrocytic glioma: genetics, biology, and paths to treatment. Genes Dev 2007; 21: 2683-710.

[3] Maher EA, Brennan C, Wen PY, Durso L, Ligon KL, Richardson A, Khatry D, Feng B, Sinha R, Louis DN, Quackenbush J, Black PM, Chin L, DePinho RA. Marked genomic differences characterize primary and secondary glioblastoma subtypes and identify two distinct molecular and clinical secondary glioblastoma entities. Cancer Res 2006; 66: 11502-13.

[4] Verhaak RG, Hoadley KA, Purdom E, Wang V, Qi Y, Wilkerson MD, Miller CR, Ding L, Golub T, Mesirov JP, Alexe G, Lawrence M, O'Kelly M, Tamayo P, Weir BA, Gabriel S, Winckler W, Gupta S, Jakkula L, Feiler HS, Hodgson JG, James CD, Sarkaria JN, Brennan C, Kahn A, Spellman PT, Wilson RK, Speed TP, Gray JW, Meyerson M, Getz G, Perou CM, Hayes DN; Cancer Genome Atlas Research Network. Integrated genomic analysis identifies clinically relevant subtypes of glioblastoma characterized by abnormalities in PDGFRA, IDH1, EGFR, and NF1. Cancer Cell 2010; 17: 98-110.

[5] Dang L, White DW, Gross S, Bennett BD, Bittinger MA, Driggers EM, Fantin VR, Jang HG, Jin S, Keenan MC, Marks KM, Prins RM, Ward PS, Yen KE, Liau LM, Rabinowitz JD, Cantley LC, Thompson CB, Vander Heiden MG, Su SM. Cancer-associated IDH1 mutations produce 2-hydroxyglutarate. Nature 2009; 462: 739-744.

[6] Wakabayashi T, Natsume A, Hatano H, Fujii M, Shimato S, Ito M, Ohno M, Ito S, Ogura M, Yoshida J. p16 promoter methylation in the serum as a basis for the molecular diagnosis of gliomas. Neurosurgery 2009; 64: 455-461; discussion 461-452.

[7] Oakhill JS, Steel R, Chen ZP, Scott JW, Ling N, Tam S, Kemp BE. AMPK is a direct adenylate charge-regulated protein kinase. Science 2011; 332: 1433-1435.

[8] Hemminki A, Markie D, Tomlinson I, Avizienyte E, Roth S, Loukola A, Bignell G, Warren W, Aminoff M, Höglund P, Järvinen H, Kristo P, Pelin K, Ridanpää M, Salovaara R, Toro T, Bodmer W, Olschwang S, Olsen AS, Stratton MR, de la Chapelle A, Aaltonen LA. A serine/threonine kinase gene defective in Peutz-Jeghers syndrome. Nature 1998; 391: 184-187.

[9] Wingo SN, Gallardo TD, Akbay EA, Liang MC, Contreras CM, Boren T, Shimamura T, Miller DS, Sharpless NE, Bardeesy N, Kwiatkowski DJ, Schorge JO, Wong KK, Castrillon DH. Somatic LKB1 mutations promote cervical cancer progression. PLoS One 2009; 4: e5137.

[10] Sanchez-Cespedes M, Parrella P, Esteller M, Nomoto S, Trink B, Engles JM, Westra WH, Herman JG, Sidransky D. Inactivation of LKB1/STK11 is a common event in adenocarcino-

mas of the lung. Cancer Res 2002; 62: 3659-3662.
[11] Bignell GR, Barfoot R, Seal S, Collins N, Warren W, Stratton MR. Low frequency of somatic mutations in the LKB1/Peutz-Jeghers syndrome gene in sporadic breast cancer. Cancer Res 1998; 58: 1384-1386.
[12] Wang J, Zhang K, Wang J, Wu X, Liu X, Li B, Zhu Y, Yu Y, Cheng Q, Hu Z, Guo C, Hu S, Mu B, Tsai CH, Li J, Smith L, Yang L, Liu Q, Chu P, Chang V, Zhang B, Wu M, Jiang X, Yen Y. Underexpression of LKB1 tumor suppressor is associated with enhanced Wnt signaling and malignant characteristics of human intrahepatic cholangiocarcinoma. Oncotarget 2015; 6: 18905-18920.
[13] Wei C, Amos CI, Stephens LC, Campos I, Deng JM, Behringer RR, Rashid A, Frazier ML. Mutation of Lkb1 and p53 genes exert a cooperative effect on tumorigenesis. Cancer Res 2005; 65: 11297-11303.
[14] Huang X, Wullschleger S, Shpiro N, McGuire VA, Sakamoto K, Woods YL, McBurnie W, Fleming S, Alessi DR. Important role of the LKB1-AMPK pathway in suppressing tumorigenesis in PTEN-deficient mice. Biochem J 2008; 412: 211-21.
[15] Morton JP, Jamieson NB, Karim SA, Athineos D, Ridgway RA, Nixon C, McKay CJ, Carter R, Brunton VG, Frame MC, Ashworth A, Oien KA, Evans TR, Sansom OJ. LKB1 haploinsufficiency cooperates with Kras to promote pancreatic cancer through suppression of p21-dependent growth arrest. Gastroenterology 2010; 139: 586-597, 597, e581-586.
[16] Calles A, Sholl LM, Rodig SJ, Pelton AK, Hornick JL, Butaney M, Lydon C, Dahlberg SE, Oxnard GR, Jackman DM, Jänne PA. Immunohistochemical loss of LKB1 is a biomarker for more aggressive biology in KRAS-mutant lung adenocarcinoma. Clin Cancer Res 2015; 21: 2851-60.
[17] Gilmore AP, Romer LH. Inhibition of focal adhesion kinase (FAK) signaling in focal adhesions decreases cell motility and proliferation. Mol Biol Cell 1996; 7: 1209-1224.
[18] Kline ER, Shupe J, Gilbert-Ross M, Zhou W, Marcus AI. LKB1 represses focal adhesion kinase (FAK) signaling via a FAK-LKB1 complex to regulate FAK site maturation and directional persistence. J Biol Chem 2013; 288: 17663-74.
[19] Huang J, Chen H, Wei Q, Zhang Z, Zhong Z, Xu Y. Downregulation of LKB1 promotes tumor progression and predicts unfavorable prognosis in patients with glioma. Oncol Lett 2017; 13: 1688-1694.
[20] Zhang K, Wang J, Yang L, Yuan YC, Tong TR, Wu J, Yun X, Bonner M, Pangeni R, Liu Z, Yuchi T, Kim JY, Raz DJ. Targeting histone methyltransferase G9a inhibits growth and Wnt signaling pathway by epigenetically regulating HP1alpha and APC2 gene expression in non-small cell lung cancer. Mol Cancer 2018; 17: 153.
[21] Zhang K, Gao H, Wu X, Wang J, Zhou W, Sun G, Wang J, Wang Y, Mu B, Kim C, Chu P, Ho DM, Ann DK, Wong TT, Yen Y. Frequent overexpression of HMGA2 in human atypical teratoid/rhabdoid tumor and its correlation with let-7a3/let-7b miRNA. Clin Cancer Res 2014; 20: 1179-1189.
[22] Zhang K, Chu K, Wu X, Gao H, Wang J, Yuan YC, Loera S, Ho K, Wang Y, Chow W, Un F, Chu P, Yen Y. Amplification of FRS2 and activation of FGFR/FRS2 signaling pathway in high-grade liposarcoma. Cancer Res 2013; 73: 1298-307.
[23] Zhang K, Wang J, Tong TR, Wu X, Nelson R, Yuan YC, Reno T, Liu Z, Yun X, Kim JY, Salgia R, Raz DJ. Loss of H2B monoubiquitination is associated with poor-differentiation and enhanced malignancy of lung adenocarcinoma. Int J Cancer 2017; 141: 766-777.
[24] Subramanian A, Tamayo P, Mootha VK, Mukherjee S, Ebert BL, Gillette MA, Paulovich A, Pomeroy SL, Golub TR, Lander ES, Mesirov JP. Gene set enrichment analysis: a knowledge-based approach for interpreting genome-wide expression profiles. Proc Natl Acad Sci U S A 2005; 102: 15545-15550.
[25] Lee MS, Jeong MH, Lee HW, Han HJ, Ko A, Hewitt SM, Kim JH, Chun KH, Chung JY, Lee C, Cho H, Song J. PI3K/AKT activation induces PTEN ubiquitination and destabilization accelerating tumourigenesis. Nat Commun 2015; 6: 7769.
[26] Zhang K, Keymeulen S, Nelson R, Tong TR, Yuan YC, Yun X, Liu Z, Lopez J, Raz DJ, Kim JY. Overexpression of flap endonuclease 1 correlates with enhanced proliferation and poor prognosis of non-small-cell lung cancer. Am J Pathol 2018; 188: 242-251.
[27] Mehenni H, Lin-Marq N, Buchet-Poyau K, Reymond A, Collart MA, Picard D, Antonarakis SE. LKB1 interacts with and phosphorylates PTEN: a functional link between two proteins involved in cancer predisposing syndromes. Hum Mol Genet 2005; 14: 2209-19.
[28] Mirouse V, Swick LL, Kazgan N, St Johnston D, Brenman JE. LKB1 and AMPK maintain epithelial cell polarity under energetic stress. J Cell Biol 2007; 177: 387-92.
[29] Carretero J, Shimamura T, Rikova K, Jackson AL, Wilkerson MD, Borgman CL, Buttarazzi MS, Sanofsky BA, McNamara KL, Brandstetter KA, Walton ZE, Gu TL, Silva JC, Crosby K, Shapiro GI, Maira SM, Ji H, Castrillon DH, Kim CF, García-Echeverría C, Bardeesy N, Sharpless NE, Hayes ND, Kim WY, Engelman JA, Wong KK.

Integrative genomic and proteomic analyses identify targets for Lkb1-deficient metastatic lung tumors. Cancer Cell 2010; 17: 547-59.
[30] Chen HC, Appeddu PA, Parsons JT, Hildebrand JD, Schaller MD, Guan JL. Interaction of focal adhesion kinase with cytoskeletal protein talin. J Biol Chem 1995; 270: 16995-9.
[31] Reis RM, Konu-Lebleblicioglu D, Lopes JM, Kleihues P, Ohgaki H. Genetic profile of gliosarcomas. Am J Pathol 2000; 156: 425-32.
[32] Ji H, Ramsey MR, Hayes DN, Fan C, McNamara K, Kozlowski P, Torrice C, Wu MC, Shimamura T, Perera SA, Liang MC, Cai D, Naumov GN, Bao L, Contreras CM, Li D, Chen L, Krishnamurthy J, Koivunen J, Chirieac LR, Padera RF, Bronson RT, Lindeman NI, Christiani DC, Lin X, Shapiro GI, Jänne PA, Johnson BE, Meyerson M, Kwiatkowski DJ, Castrillon DH, Bardeesy N, Sharpless NE, Wong KK. LKB1 modulates lung cancer differentiation and metastasis. Nature 2007; 448: 807-810.
[33] Liu W, Monahan KB, Pfefferle AD, Shimamura T, Sorrentino J, Chan KT, Roadcap DW, Ollila DW, Thomas NE, Castrillon DH, Miller CR, Perou CM, Wong KK, Bear JE, Sharpless NE. LKB1/STK11 inactivation leads to expansion of a prometastatic tumor subpopulation in melanoma. Cancer Cell 2012; 21: 751-64.
[34] Sakamoto S, McCann RO, Dhir R, Kyprianou N. Talin1 promotes tumor invasion and metastasis via focal adhesion signaling and anoikis resistance. Cancer Res 2010; 70: 1885-95.
[35] Lifschitz-Mercer B, Czernobilsky B, Feldberg E, Geiger B. Expression of the adherens junction protein vinculin in human basal and squamous cell tumors: relationship to invasiveness and metastatic potential. Hum Pathol 1997; 28: 1230-1236.
[36] Asada N, Sanada K, Fukada Y. LKB1 regulates neuronal migration and neuronal differentiation in the developing neocortex through centrosomal positioning. J Neurosci 2007; 27: 11769-11775.
[37] Wen PY, Lee EQ, Reardon DA, Ligon KL, Alfred Yung WK. Current clinical development of PI3K pathway inhibitors in glioblastoma. Neuro Oncol 2012; 14: 819-829.
[38] Faivre S, Kroemer G, Raymond E. Current development of mTOR inhibitors as anticancer agents. Nat Rev Drug Discov 2006; 5: 671-688.
[39] Shackelford DB, Abt E, Gerken L, Vasquez DS, Seki A, Leblanc M, Wei L, Fishbein MC, Czernin J, Mischel PS, Shaw RJ. LKB1 inactivation dictates therapeutic response of non-small cell lung cancer to the metabolism drug phenformin. Cancer Cell 2013; 23: 143-58.
[40] Shorning BY, Griffiths D, Clarke AR. Lkb1 and Pten synergise to suppress mTOR-mediated tumorigenesis and epithelial-mesenchymal transition in the mouse bladder. PLoS One 2011; 6: e16209.
[41] Tanwar PS, Mohapatra G, Chiang S, Engler DA, Zhang L, Kaneko-Tarui T, Ohguchi Y, Birrer MJ, Teixeira JM. Loss of LKB1 and PTEN tumor suppressor genes in the ovarian surface epithelium induces papillary serous ovarian cancer. Carcinogenesis 2014; 35: 546-553.
[42] Cheng H, Liu P, Zhang F, Xu E, Symonds L, Ohlson CE, Bronson RT, Maira SM, Di Tomaso E, Li J, Myers AP, Cantley LC, Mills GB, Zhao JJ. A genetic mouse model of invasive endometrial cancer driven by concurrent loss of Pten and Lkb1 Is highly responsive to mTOR inhibition. Cancer Res 2014; 74: 15-23.
[43] Shackelford DB, Abt E, Gerken L, Vasquez DS, Seki A, Leblanc M, Wei L, Fishbein MC, Czernin J, Mischel PS, Shaw RJ. LKB1 inactivation dictates therapeutic response of non-small cell lung cancer to the metabolism drug phenformin. Cancer Cell 2013; 23: 143-58.
[44] Carmignani M, Volpe AR, Aldea M, Soritau O, Irimie A, Florian IS, Tomuleasa C, Baritchii A, Petrushev B, Crisan G, Valle G. Glioblastoma stem cells: a new target for metformin and arsenic trioxide. J Biol Regul Homeost Agents 2014; 28: 1-15.

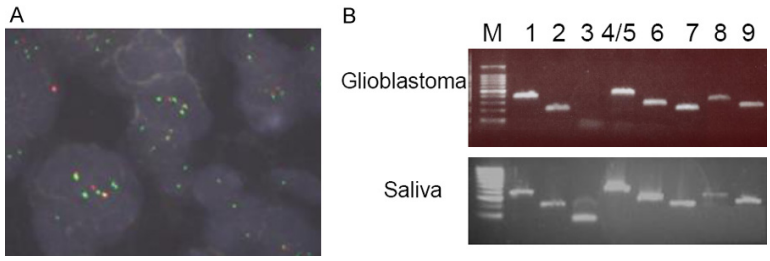

Figure S1. A. Dual-color FISH analysis showed that more that the majority of cells in these tissues displayed 1R/2G or 0R/2G patterns. B. Gel electrophoresis analysis of the PCR products revealed lack of amplified products of exon 3 of LKB1 gene in genome of gliosarcoma not that of saliva (1 to 9 for exon 1-9).

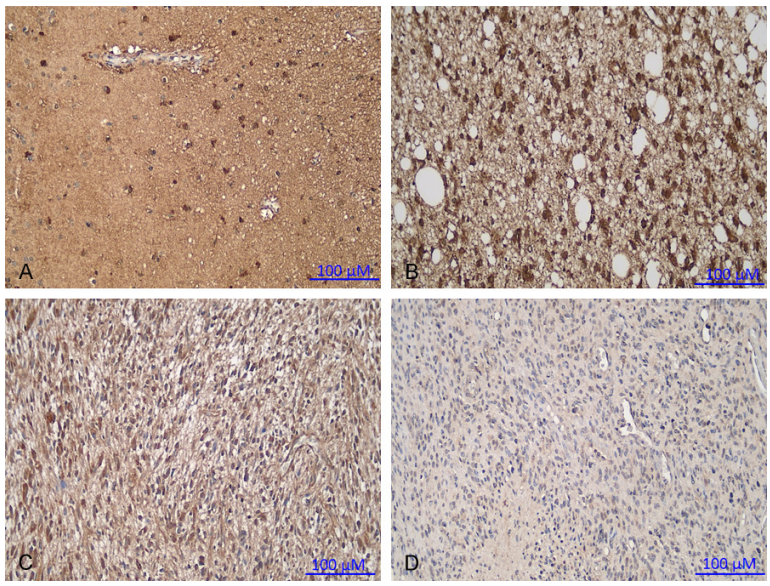

Figure S2. Photomicrographs of IHC analysis of LKB1 in normal brain and glioma. A. Normal brain; B. Astrocytoma; C. Anaplastic Astrocytoma; D. GBM.

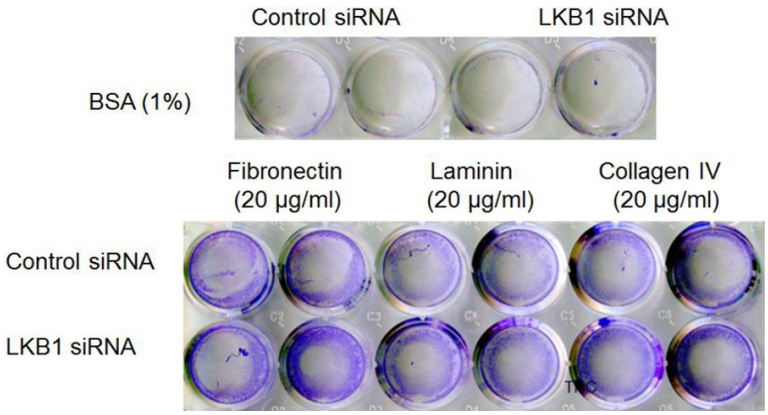

Figure S3. Knockdown of LKB1 decrease the adhesion of T98 cells to extracellular matrix components. Following knockdown of LKB1 72 h, the adhesion of T98 cells to fibronectin, laminin I, collagen I, collagen IV and fibrinogen were analyzed by cell adhesion assay, with BSA (upper panel) as the control.

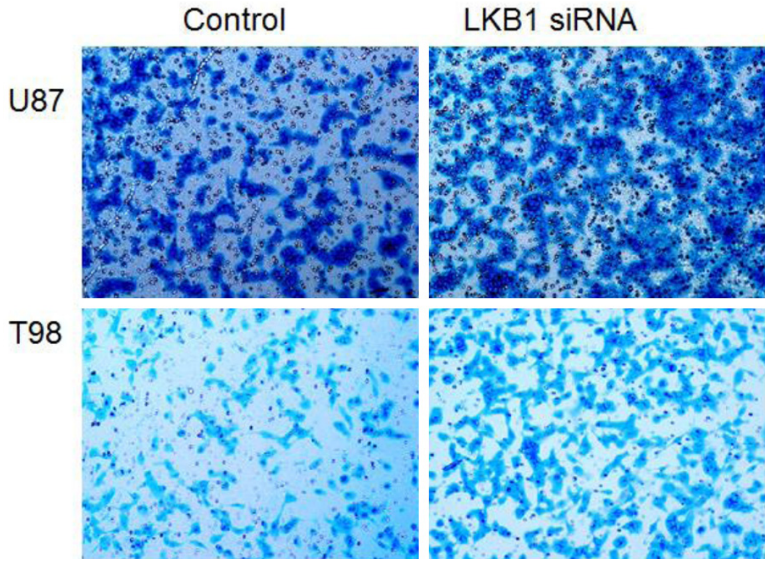

Figure S4. Knockdown of LKB1 increased the migration of T98 cells to extracellular matrix components. Following knockdown of LKB1 72 h, the migration of glioblastoma cells were analyzed by cell migration assay, and representative images of migrating cells were shown, magnification ×100.

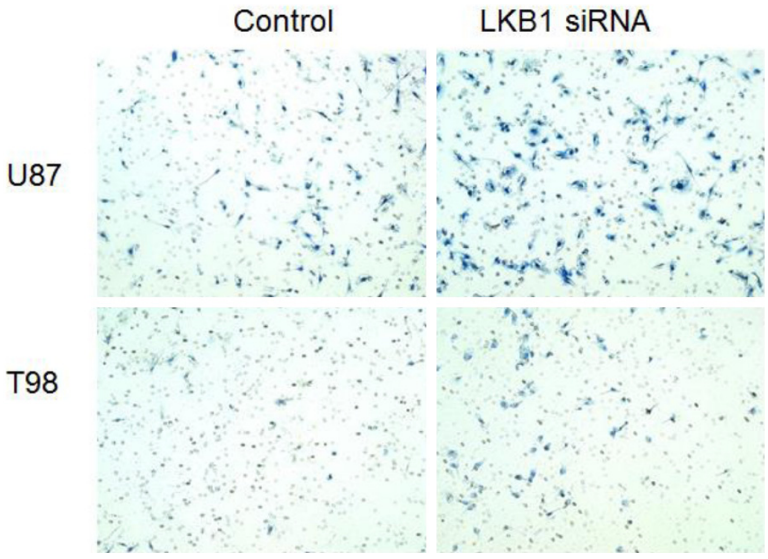

Figure S5. LKB1 knockdown of LKB1 enhanced the invasiveness of glioblastoma cells. U87 and T98 cells were treated with LKB1 siRNA for 72 h, with the control siRNA as the negative control. The invasion of cells was measured by Matrigel invasion assay. Representative invasive cells were shown, magnification, ×100.

Table S1. Differentially expressed genes in T98 and U87 glioblastoma cells upon LKB1 knockdown

Gene symbol	T98		U87	
	log2FC*	adj.P.Val	log2FC*	adj.P.Val
SCML2	-4.03045	8.07E-28	-2.78	1.05E-20
VCL	-3.63387	1.50E-52	-1.98	1.88E-17
BAGE2	-3.12316	7.00E-16	1.55	2.79E-05
BAGE3	-3.12316	7.00E-16	1.55	2.79E-05
PTX3	-3.11638	2.52E-36	-1.73	1.37E-12
BAGE4	-3.07164	2.97E-15	1.51	4.69E-05
BAGE5	-3.07164	2.97E-15	1.51	4.69E-05
CLDN12	-2.6057	3.99E-27	-1.87	1.59E-14
STK11	-2.60306	1.48E-26	-2.74	2.19E-28
CCDC99	-2.50516	1.13E-26	-1.88	8.10E-15
GBE1	-2.49539	5.71E-27	-1.26	1.47E-07
GXYLT1	-2.47513	9.44E-24	-2.25	1.23E-20
SNAP23	-2.35063	4.75E-22	-1.61	6.21E-11
KIAA0754	-2.34673	5.88E-20	1.77	7.71E-13
RCHY1	-2.34593	1.55E-18	-1.22	7.27E-06
RBMS1	-2.29758	2.32E-23	-1.39	6.03E-09
RNF19B	-2.2786	3.90E-19	-1.04	0.000134
BIRC3	-2.22452	6.72E-22	-1.06	9.24E-05
SGMS1	-2.19718	1.62E-17	-1.08	2.44E-05
FERMT2	-2.18688	6.20E-20	-1.83	2.68E-14
C4orf34	-2.14345	2.21E-16	-1.79	3.59E-12
RAB11FIP2	-2.1399	3.16E-16	-1.20	3.24E-06
CPOX	-2.13676	3.00E-19	-1.33	5.56E-08
PTPRJ	-2.11665	3.41E-20	-1.02	5.12E-05
HMMR	-2.05555	6.06E-19	-2.39	2.37E-23

TTL	-2.00931	1.70E-17	-2.07	1.25E-18
SGPP1	-1.96431	3.03E-12	-1.10	2.13E-05
IPMK	-1.96047	1.54E-15	-1.03	0.000136
DPYSL3	-1.9539	1.53E-17	-1.15	3.52E-06
RAB31	-1.95011	2.96E-17	-2.06	5.08E-19
TSPYL4	-1.93466	2.84E-13	-1.16	5.72E-06
SGK3	-1.88548	1.21E-09	-1.58	8.44E-09
EFHA2	-1.88289	2.93E-08	-1.31	1.89E-05
ESYT2	-1.87023	5.18E-16	-1.34	1.75E-08
RAB8A	-1.85566	2.66E-15	-1.49	6.00E-10
SCARB2	-1.84986	1.32E-15	-1.23	3.06E-07
ZSWIM4	-1.82812	1.33E-11	-1.22	4.40E-06
VASN	-1.82675	3.18E-14	-1.47	7.49E-09
FJX1	-1.78208	5.78E-14	-1.06	3.11E-05
ENC1	-1.76383	7.44E-14	-1.12	6.20E-06
AHCYL2	-1.75061	2.53E-11	-1.53	5.59E-10
CENPF	-1.74731	2.50E-14	-1.30	1.04E-07
RREB1	-1.74394	8.44E-13	-1.10	0.000136
FBXO45	-1.73275	1.13E-13	-1.11	3.28E-05
8-Mar	-1.72236	2.38E-07	-1.05	0.000253
SPRYD3	-1.71853	2.14E-12	-1.39	5.60E-09
METAP2	-1.71174	1.47E-13	-1.27	4.67E-07
C8orf44-SGK3	-1.71001	2.52E-08	-1.46	9.15E-08
AP1AR	-1.69062	5.63E-11	-1.45	3.24E-08
SAMD10	-1.68316	0.000494	-1.07	0.003932
POLQ	-1.66463	1.57E-12	-1.24	5.77E-06
KIAA1147	-1.65647	8.45E-12	-1.37	4.01E-08
C14orf129	-1.64296	9.97E-10	-1.28	4.45E-07
CDK6	-1.64188	7.54E-13	-1.13	4.50E-06
MTMR9	-1.62308	1.98E-11	-1.12	7.23E-06
SGPL1	-1.6117	2.04E-11	-1.51	1.09E-09
NRAS	-1.59446	6.42E-12	-1.43	1.54E-09
ID2	-1.59411	1.82E-10	-1.74	1.92E-13
DDX60	-1.58743	1.78E-10	-1.65	6.16E-08
ACVR2B	-1.58422	9.93E-09	-1.09	0.00033
PIP5K1A	-1.58063	1.06E-11	-1.11	9.07E-06
SEL1L	-1.5408	1.28E-10	-1.30	7.61E-08
BLOC1S5	-1.52744	2.24E-09	-1.31	6.56E-06
C17orf97	-1.50222	9.18E-05	-1.80	1.70E-05
SETD8	-1.48524	6.15E-10	-1.89	1.70E-14
RBM47	-1.48444	1.55E-08	-1.38	4.79E-07
WBP1L	-1.4753	1.06E-09	-1.07	1.89E-05
FBXO33	-1.47213	1.88E-08	-1.03	0.000133
VPS36	-1.46963	8.74E-10	-1.32	3.27E-07
SESTD1	-1.44709	1.21E-09	-1.17	3.94E-06
H1F0	-1.44664	5.55E-10	-1.01	9.50E-05
ERI1	-1.41793	4.44E-09	-1.03	9.12E-05
TNFAIP2	-1.3586	1.15E-08	-1.45	1.73E-09
SOGA1	-1.34947	1.02E-08	1.16	2.48E-06

PHF7	-1.33714	0.000427	-1.37	0.000128
C3AR1	-1.33242	0.003114	-1.27	1.74E-06
APLF	-1.32818	0.000209	-1.43	1.54E-05
CHN1	-1.32785	7.26E-08	-2.56	3.99E-22
ZNF367	-1.31336	8.31E-08	-2.79	2.07E-27
CDPF1	-1.31316	5.34E-06	-1.56	3.19E-05
MILR1	-1.31054	0.001082	-1.13	0.002807
GLRB	-1.29864	0.000473	-1.38	4.37E-06
DERA	-1.29777	1.44E-07	-1.13	6.60E-06
SH3YL1	-1.29496	0.004632	-1.58	2.81E-08
POLR3GL	-1.28445	8.98E-07	-1.34	5.01E-07
DONSON	-1.27237	1.43E-07	-1.84	4.75E-12
PSIP1	-1.27198	1.47E-07	-1.14	6.51E-06
CEP44	-1.2584	1.58E-06	-1.34	2.54E-07
VMA21	-1.24771	2.65E-07	-1.17	2.49E-06
SLC17A5	-1.23891	4.52E-06	-1.28	6.12E-07
MNS1	-1.23424	6.51E-06	-1.51	7.41E-07
RFWD3	-1.23028	1.79E-07	-1.13	6.60E-06
G3BP1	-1.22346	1.87E-07	-1.01	6.09E-05
LOC81691	-1.22266	5.62E-06	-1.59	3.24E-09
MDN1	-1.21517	4.21E-07	1.13	1.07E-05
NEIL3	-1.21141	3.28E-07	-1.67	4.93E-10
RTN3	-1.20384	3.29E-07	-1.49	2.52E-10
PM20D2	-1.20214	2.86E-05	-1.64	6.37E-09
MAT2B	-1.1996	5.40E-07	-1.11	1.09E-05
SFMBT1	-1.18936	1.91E-06	-1.13	7.50E-05
CNTRL	-1.18826	1.98E-06	-1.23	4.82E-06
SCML1	-1.18105	9.04E-07	-1.78	1.43E-12
KIF14	-1.17676	9.00E-07	-1.10	7.73E-05
IGIP	-1.1763	0.005326	-1.29	0.000163
NBPF1	-1.17608	1.23E-05	1.13	8.19E-05
LYN	-1.17221	1.02E-06	-1.27	0.00287
NUDT19	-1.16433	1.66E-05	-1.08	0.000115
MAP3K3	-1.16331	2.06E-06	-1.18	4.78E-06
HOXA1	-1.15949	0.001158	-1.17	0.000363
TTC7B	-1.15855	0.000125	-1.12	3.11E-05
FMNL1	-1.15322	1.12E-05	-1.35	4.41E-05
INIP	-1.15129	2.54E-05	-1.47	7.15E-08
TMX1	-1.15057	1.85E-06	-1.09	1.33E-05
NLRX1	-1.1501	5.16E-05	-1.32	0.000357
DLGAP5	-1.14573	1.89E-06	-1.75	5.14E-13
CFL2	-1.14155	3.38E-06	-1.20	1.06E-06
C14orf142	-1.13322	0.0002	-1.08	0.000128
CLSPN	-1.13258	2.96E-06	-1.11	2.44E-05
BRCA1	-1.12935	2.41E-06	-1.13	1.20E-05
MYBL1	-1.12247	7.24E-06	-1.20	4.27E-06
TBX2	-1.11831	0.000231	1.26	1.96E-06
KIF20B	-1.11522	3.33E-06	-1.16	5.10E-06
ERI2	-1.11132	1.33E-05	-1.46	1.10E-08

APOLD1	-1.10629	0.00021	-1.28	6.56E-06
GAS2L3	-1.09921	2.34E-05	-1.53	1.81E-06
CASC5	-1.09634	6.73E-06	-1.19	6.20E-06
CLIP4	-1.08332	9.15E-06	-1.31	1.17E-07
MBIP	-1.06609	8.23E-05	-1.08	0.000313
GPR176	-1.06181	2.30E-05	-1.04	8.63E-05
NUS1	-1.0543	1.21E-05	-1.03	3.72E-05
SVIP	-1.0496	0.000512	-1.62	3.61E-10
C4orf21	-1.03305	5.32E-05	-1.34	5.58E-06
DEPDC1	-1.03257	1.78E-05	-2.14	4.33E-19
LRRCC1	-1.02889	0.000153	-1.42	8.40E-07
WHSC1	-1.0113	2.50E-05	-1.04	2.63E-05
KIF23	-1.00876	2.76E-05	-1.67	3.32E-12
COMMD10	-1.00228	9.62E-05	-1.00	0.000314
GOPC	1.004086	4.20E-05	1.11	7.52E-06
SLC35D1	1.00447	4.31E-05	1.10	1.31E-05
RAB3A	1.007594	0.025167	1.18	0.002662
CLIC4	1.020522	2.09E-05	1.45	6.00E-10
USP15	1.024016	4.06E-05	1.10	1.33E-05
EDIL3	1.032402	7.13E-05	1.79	6.88E-14
HERPUD2	1.033689	9.01E-05	1.03	9.93E-05
FTSJ1	1.051114	2.50E-05	1.13	6.27E-06
MPP2	1.067784	8.54E-05	1.19	1.97E-06
VGLL4	1.078371	8.57E-06	1.02	4.12E-05
VCAN	1.114464	1.39E-05	1.66	1.55E-12
LUZP6	1.116031	2.44E-06	1.02	3.32E-05
MTPN	1.116031	2.44E-06	1.02	3.32E-05
CDC14A	1.116051	9.07E-05	1.43	2.91E-06
PAWR	1.117354	1.04E-05	1.29	0.000997
CASK	1.134519	1.76E-05	1.02	7.35E-05
SS18L1	1.146467	7.12E-06	1.24	2.05E-06
AKAP8	1.168394	2.45E-06	1.08	4.54E-05
TK2	1.171939	2.46E-05	1.22	8.86E-07
SATB2	1.199266	1.73E-05	1.11	1.44E-05
TLN1	1.20675	2.95E-07	2.18	4.76E-21
TFAP2C	1.212228	7.82E-07	1.26	0.002507
TPBG	1.244602	2.95E-07	1.70	4.19E-13
HMOX1	1.252769	1.10E-07	1.41	2.54E-09
SPOPL	1.259562	1.22E-06	1.38	6.06E-08
NR2F2	1.287725	8.63E-08	1.22	1.56E-06
GPR3	1.297599	8.43E-05	1.29	1.94E-06
SLC16A2	1.301293	3.57E-08	1.14	3.15E-06
ICOSLG	1.308755	1.45E-07	1.11	2.31E-05
PTP4A1	1.314171	2.35E-08	1.35	1.67E-08
MTFP1	1.317574	7.59E-08	1.04	0.000146
TDO2	1.325646	0.000129	1.14	3.25E-05
NT5DC2	1.341431	1.21E-08	1.87	1.01E-15
IL6ST	1.34234	7.23E-09	2.37	3.32E-24
SLC6A9	1.351114	4.27E-08	1.06	0.000781

ELFN2	1.363303	2.28E-08	2.02	1.43E-12
MCF2L	1.373607	1.36E-07	1.23	1.81E-06
XYLT1	1.377755	2.15E-08	1.21	4.45E-07
DUSP6	1.387675	8.57E-06	1.20	1.10E-06
DHX40	1.401491	5.72E-09	1.67	3.32E-12
HPS6	1.403029	1.65E-08	1.01	0.000158
FAM49A	1.412228	5.33E-05	1.35	3.01E-05
C6orf70	1.412987	4.18E-07	1.15	4.39E-05
EHD3	1.435405	3.36E-07	1.05	3.69E-05
PPP1R14B	1.440264	6.47E-10	1.19	1.29E-06
SAR1B	1.493817	2.23E-10	1.51	3.61E-10
EPHA4	1.526519	6.72E-11	2.08	1.37E-12
CYB5R4	1.537707	6.51E-10	1.47	2.03E-08
ASPHD1	1.540572	1.78E-09	1.09	4.67E-05
ZCCHC3	1.556595	4.19E-11	1.42	1.42E-07
TMEM41A	1.568231	1.20E-10	1.43	3.99E-08
HOMER1	1.574932	1.20E-09	2.05	3.18E-14
TMEM115	1.577474	3.45E-11	1.01	6.09E-05
MFSD2A	1.58398	1.97E-08	1.55	7.39E-10
TNC	1.663951	3.30E-12	1.71	1.60E-13
HSPA6	1.695139	7.49E-06	1.07	0.018818
CSGALNACT1	1.714664	1.33E-07	1.80	1.75E-13
TSPAN15	1.750629	0.00134	-1.64	1.27E-06
PANK3	1.754376	1.09E-13	2.72	1.57E-27
CITED2	1.761661	4.87E-14	1.16	2.67E-06
MOGS	1.774717	9.39E-14	1.53	1.05E-10
SLC41A1	1.776467	4.42E-14	2.08	1.88E-17
IL10RB	1.840551	7.97E-15	1.53	4.77E-10
TGM2	1.857998	2.98E-14	2.12	7.54E-20
POLR3E	1.874886	6.04E-15	1.97	9.93E-15
LSM14A	1.909474	3.12E-16	1.80	5.95E-14
IQSEC1	1.941607	1.01E-12	1.52	1.34E-09
DUSP5	1.953693	2.44E-15	1.21	1.57E-06
YWHAH	1.969076	1.57E-17	1.38	8.71E-09
DISP2	1.979515	2.32E-14	1.27	0.000128
SNRNP27	2.041326	6.82E-16	1.46	9.16E-09
ANO10	2.042558	3.42E-17	1.80	3.36E-14
GDF15	2.097061	9.04E-19	1.11	1.21E-05
ALCAM	2.099813	2.94E-19	2.72	6.90E-30
HIPK3	2.123469	1.55E-18	2.44	3.99E-22
OSGIN2	2.132095	1.63E-18	2.09	2.13E-18
BEX1	2.164658	9.20E-07	1.38	0.000127
CA9	2.172101	1.65E-08	1.00	5.06E-05
MEST	2.177537	5.08E-21	2.29	1.13E-22
SYT11	2.261774	1.10E-17	1.26	1.41E-07
THG1L	2.265015	3.72E-17	1.77	2.18E-08
RASD2	2.281449	1.15E-09	1.81	3.45E-07
SNAP25	2.298293	1.08E-15	1.63	1.78E-11
NUDT15	2.393362	2.58E-22	1.58	8.99E-08

HS6ST1	2.423095	1.46E-24	1.91	9.72E-13
ISM1	2.497685	1.18E-10	1.56	1.81E-06
SCN1B	2.574917	4.46E-08	1.85	4.84E-06
EMP2	2.714693	7.18E-30	1.62	2.43E-11
GDF11	2.752306	4.23E-27	2.23	1.84E-19
STEAP3	2.778595	3.77E-31	2.00	7.34E-18
4-Mar	2.778923	2.42E-15	1.39	4.46E-06
TOP1MT	2.794957	1.14E-27	2.00	1.92E-13
RPS26	3.047433	1.78E-30	1.47	4.59E-09
SYP	3.101358	1.57E-23	1.50	1.28E-05
SCG2	3.112957	9.33E-35	1.73	1.53E-12
CHPF	3.325909	7.32E-44	2.66	1.62E-29
KRTAP1-5	3.339525	1.05E-09	2.65	1.77E-06
KIF5C	3.500272	8.07E-28	1.11	6.96E-06
VGF	3.570113	1.11E-28	2.05	5.77E-16
PIANP	3.81061	1.17E-18	1.50	4.77E-09
CEND1	5.382637	2.91E-64	1.32	7.18E-08

*The mRNA expression levels of genes in LKB1-attenuated glioblastoma cells are presented as log2 ratio to that of glioblastoma cells transfected with control siRNA. If the absolute log2 ratio of 2 cells were no less than 1.0, the gene would be listed.

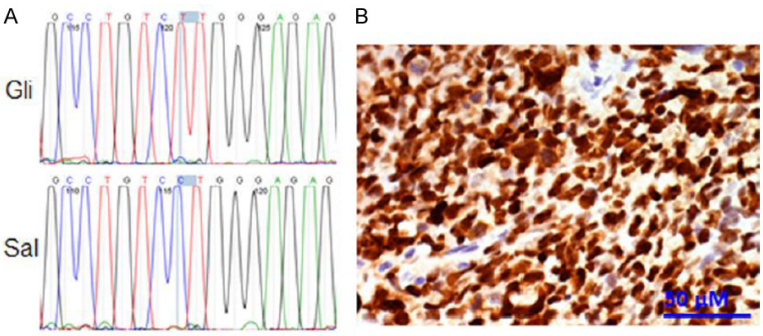

Figure S6. Identification of inactivation of p53 in the glioblastoma. A. Sanger sequencing showed the missense mutation c883T P278L in the genome. B. IHC for p53 shows extremely strong homogenous in tumor cells compared to the retained staining of nuclei of vascular cells.